Pulmonary Infections – Pneumonia

13

Roger Eibel

CONTENTS

KEY POINTS

The different appearances of pneumonia such as ill-defined nodules, ground-glass opacities, and consolidations can be easily detected and differentiated with MRI. Since very small nodules and calcifications are extremely challenging due to rather thick slices and loss of signal, MRI is highly recommended as a follow-up tool, to avoid repetitive investigations using ionizing radiation. With the sensitivity of T2-weighted sequences and the potential of contrast-enhanced T1-weighted sequences important differential diagnostic considerations can be provided. Additionally, developing complications, such as pericardial or pleural effusions, empyema or lung abscess, are easily recognized. Current and future studies are to demonstrate that MRI is well suited as a monitoring and follow-up tool during and after therapy and compares favorably with CT or other imaging methods regarding sensitivity and specificity.

13.1
Definition

Pneumonia is an infection of the gas-exchanging units of the lung, caused most commonly by bacteria but occasionally by viruses, fungi, parasites, and other infectious agents.

Pneumonia is the sixth leading cause of death in the United States, and the leading cause of death from infectious disease (Niederman et al. 2001). In hospitalized patients, particularly those who are mechanically ventilated, pneumonia is the leading cause of death from nosocomial infection (Campbell et al. 1996).

R. Eibel, MD
Chief of the Department of Radiology and Neuroradiology, HELIOS Clinics Schwerin, Teaching Hospital of the University of Rostock, Wismarsche Str. 393, 19049 Schwerin, Germany

13.2
Pathogenesis

Pneumonia can result whenever the pulmonary defense mechanisms are impaired or whenever the resistance of the host in general is lowered. Factors that affect resistance in general include:
- Chronic diseases
- Immunologic deficiency
- Treatment with immunosuppressive agents
- Leukopenia
- Unusually virulent infections

The clearing mechanisms can be interfered with by many factors, such as the following:
- Loss or suppression of the cough reflex (coma, drugs)
- Injury to the mucociliary apparatus (cigarette smoke, gas inhalation, viral diseases)
- Interference with the phagocytic or bactericidal action of alveolar macrophages (alcohol, smoke)
- Pulmonary congestion and edema
- Accumulation of secretions (cystic fibrosis, bronchial obstruction)

Some other points need to be emphasized, before listened up the different classification schemes. (1) One type of pneumonia sometimes predisposes to another, especially in debilitated patients. (2) Although the portal of entry for most pneumonias is the respiratory tract, hematogenous spread from one organ to other organs can occur. (3) Many patients with chronic disease acquire terminal pneumonias while hospitalized.

13.3
Classification

Pneumonias are classified by the specific etiologic agent, who determines the treatment, or, if no pathogen can be isolated, by the clinical setting in which the infection occurs. Below the different entities of the pneumonia syndromes are briefly discussed to clarify the terms and the characteristics and the peculiarities.

13.3.1
Community Acquired Acute Pneumonia (CAP)

CAP may be bacterial or viral. Often, the bacterial infection follows an upper respiratory tract viral infection.

Bacterial invasion of the lung parenchyma causes the alveoli to be filled with an inflammatory exudate, thus causing consolidation of the pulmonary tissue (HUSAIN and KUMAR 2005). Predisposing conditions include extremes of:
- Age
- Chronic diseases (congestive heart failure, COPD, and diabetes)
- Congenital or acquired immune deficiencies
- Decreased or absent splenic function (post splenectomy, sickle cell disease)

It is beyond the scope of this book chapter, to describe the different pneumonias caused by various organisms, but with regard to magnetic resonance imaging it is necessary to mention the different morphologic features common to most pneumonias.

According to the anatomic distribution in the lung, the two major categories are lobar versus bronchopneumonia. *Lobar pneumonia* is a classic manifestation of pneumococcal pneumonia in which an entire lobe is affected by the inflammatory infiltrate, with extension up to the pleura or a major fissure. In patients with this type, the stages of pneumonia progress from:
- Edema to
- Red hepatization (alveolar fibrin, neutrophils, lymphocytes, and pneumocyte hyperplasia)
- Gray hepatization (predominantly neutrophilic infiltrates with lysis of erythrocytes and inflammatory cells)
- Resolution (organizing pneumonia, macrophages, proliferation of loose connective tissue in distal airspaces)

The basic *radiographic pattern* of this type of pneumonia is a homogeneous consolidation with or without air bronchogram. The consolidation is bounded by fissure and in contrast to an atelectasis no shrinkage or volume loss can be delineated in the acute phase.

Bronchopneumonia is also known as lobular or focal pneumonia. It is characterized by centrilobular inflammation that is concentrated around respiratory bronchioles, with spread to the surrounding alveolar ducts and alveolar spaces. When lobular pneumonia becomes confluent, it may be difficult to separate from lobar pneumonia. From a clinical standpoint it is sometimes difficult to apply these classic categories. More important for imaging is the determination of the extent of disease and the delineation of complications such as abscess formation, empyema, organization, and dissemination.

Common *radiographic findings* are nodular and patchy patterns due to involvement and sparing of acini. Sometimes volume loss can be found.

13.3.2
Community-acquired Atypical Pneumonias

The term "*atypical*" refers to the following findings:
- Moderate amount of sputum
- No physical findings of consolidation
- Only moderate evaluation of white cell count
- Lack of alveolar exudate

Most commonly this type of pneumonia is caused by *Mycoplasma pneumoniae*, viruses, and *Chlamydia pneumoniae*. These agents produce primarily an interstitial inflammation within the walls of the alveoli, resulting in thickening of the alveolar septa, later fluid accumulation and cellular exudate into the alveolar spaces. Superimposed bacterial infection modifies the histologic and the subsequent radiologic picture (Husain and Kumar 2005).

Interpreting chest films and especially CT, *radiographic patterns* which can be found in this category are peribronchial thickening, reticular and reticulonodular pattern, with filling of the acini ground-glass and sometime a crazy-paving pattern. A subsegmental collapse additional can be delineated.

13.3.3
Nosocomial Pneumonia

In 1995, the American Thoracic Society published a consensus statement defining nosocomial or hospital-acquired pneumonia (HAP) as a pneumonia that is:
- Not incubating at the time of hospital admission and
- Begins more than 48 h after admission (Campbell et al. 1996)

There are 300,000 cases of HAP annually in the United States and it carries an associated mortality of 30%–70% (McEachern and Campbell 1998). It is common in patients with severe underlying disease, prolonged antibiotics, intravascular devices, and mechanical ventilation. The last one is also termed ventilator-associated pneumonia (VAP). In a prospective study of 1014 mechanically ventilated patients, VAP developed in 177 patients. The mean time to onset was 9 days, with a median time to onset of 7 days after ICU admission. However, when the daily hazard rate of infection was calculated, it was estimated to be 3.3% at day 5, 2.3% at day 10, and 1.3% at day 15 (Cook et al. 1998). This documents a significant decline in pneumonia risk with time. Because the risk for pneumonia is so high early

after intubation, pneumonias beginning within the first 5 days (*early-onset infection*) account for 50% of all episodes of VAP, and the natural history and pathogens of this infection differ from those associated with VAP of *late onset* (Prod'hom et al. 1994). Common isolates are Gram-negative bacteria and *Staphylococcus aureus*. Typical radiologic patterns cannot be described. This is due to the different circumstances and risk factors, which contribute to the development of HAP. The other explanations are the different organisms responsible for the pneumonia. Within the first days the more common organisms are *Streptococcus pneumoniae*, *Moraxella catarrhalis*, *Staphylococcus aureus*, and *Hemophilus influenzae* (Craven and Steger 1995). Later on, Gram-negative rods predominate. The risk factors for mortality from VAP are summarized in Table 13.1.

Microaspiration of contaminated oropharyngeal secretions seems to be the most cause of HAP (McEachern and Campbell 1998). After macroaspiration another subtype of pneumonia can occur, termed *aspiration pneumonia*. This resultant pneumonia is partly chemical, owing to the extremely irritating effects of the gastric acid appearing like pulmonary edema, and partly bacterial (from the oral flora). This type of pneumonia is often necrotizing, with abscess formation is a common complication (Husain and Kumar 2005). As *radiographic patterns* in this particular type of pneumonia, patchy consolidations in the dependent portions of the lungs with a usually multilobar and bilateral distribution is common.

Diagnosing HAP is difficult because there is no method for obtaining a diagnosis that is reliable in all cases. The diagnosis is initially made on clinical grounds by the finding of a new infiltrate on chest radiograph, fever, purulent sputum, or other signs of clinical deterioration. Unfortunately, this clinical method was shown to be specific for HAP in only 27 of 84 patients in a series reported by Fagon et al. (1993) because many other conditions such as congestive heart failure, pulmonary embolism, atelectasis, ARDS, pulmonary hemorrhage, or drug reactions may mimic pneumonia, particularly in critically ill patients. While there are many different testing modalities that may be employed to this end, all have their limitations and none is sufficiently sensitive and specific to be considered a "gold standard" test (Rello et al. 2001).

13.3.4
Chronic Pneumonia

Chronic pneumonia results from granulomatous inflammation, due to bacteria (e.g. *Mycobacterium tuber-*

Table 13.1. Risk factors for an adverse outcome (mortality) from ventilator-associated pneumonia (adapted from NIEDERMAN 2004)

Patient risk factors
Historical data
Prolonged mechanical ventilation before pneumonia
Medical (vs surgical) diagnosis
Age >60 years
Physiologic factors
Underlying fatal or serious illness
Severe pneumonia (with sepsis or ARDS)
Coma on admission
Multiple system organ failure
Laboratory data
Bilateral lung infiltrates
Bacteriologic risk factors
High-risk pathogen
Pseudomonas aeruginosa
Acinetobacter species
Stenotrophomonas maltophilia
Methicillin-resistant *Staphylococcus aureus*
Antibiotic resistant pathogen, especially if acquired during therapy
Superinfection after a first course of therapy
Therapy-related risk factors
Prior antibiotic therapy
Inadequate initial therapy (organisms not sensitive to therapeutic agent)
Inadequate dose or dose regimen

culosis) or fungi (e.g. *Histoplasma capsulatum*, *Blastomyces dermatidis*, *Coccidioides immitis*). It is most often a localized lesion in the immunocompetent patient. Unlike tuberculosis, the above mentioned fungal species are geographic in that it causes disease in particular localization in the United States and in Mexico.

In the lungs these infections produce epithelioid cell granulomas, which usually undergo coagulative necrosis and coalesce to produce larger areas of consolidation. Also they can liquefy to form cavities. Spontaneously or during therapy these lesions can undergo fibrosis and concentric calcification. As a consequence the typical *radiographic appearance* of this type of pneumonia is the single or multiple lung nodules with or without calcification.

13.3.5
Pneumonia in the Immunocompromised Host

The appearance of a pulmonary infiltrates and signs of infection (e.g., fever) is one of the most common and serious complications in patients whose immune and defense systems are suppressed by disease, immunosuppression for organ transplantation and tumors, or irradiation (ROSENOW 1990).

The host defense system includes physical and chemical barriers to infection, the inflammatory response, and the immune response. Physical barriers, such as the skin and mucous membranes, prevent invasion by most organisms. Chemical barriers include lysozymes and hydrochloric acid. Lysozymes destroy bacteria by removing cell walls. Hydrochloric acid breaks down food and mucus that contains pathogens. The inflammatory response involves polymorphonuclear leukocytes, basophils, mast cells, platelets and, to some extent, monocytes and macrophages. The immune response primarily involves the interaction of lymphocytes (T and B), macrophages, and macrophage-like cells and their products. These cells may be circulating or may be localized in the immune system's tissues and organs (SPRINGHOUSE 2007). Primary immune deficiency diseases are disorders in which part of the body's immune system is missing or does not function properly. In contrast to secondary immune deficiency disease in which the immune system is compromised by factors outside the immune system, such as viruses or chemotherapy, the primary immune deficiency diseases are caused by intrinsic or genetic defects in the immune system.

Primary immunodeficiencies are complex diseases. Since each one can be traced to the failure of one or more parts of the immune system, one of the more convenient ways to group them is according to the part of the immune system that is faulty:
- B cell (antibody) deficiencies
- Combined T cell and B cell (antibody) deficiencies
- T cell deficiencies
- Defective phagocytes
- Complement deficiencies
- Deficiencies/cause unknown

Antibody deficiencies can hinder or prevent the immune system from recognizing and marking for destruction bacteria, viruses and other foreign invaders. X-linked agammaglobulinemia, an inherited deficiency that appears in the first 3 years of life, leaves infants and young children with recurrent infections of the ears, lungs, sinuses and bones, and increased susceptibility to such viruses as hepatitis and polio.

Combined immunodeficiencies occur in people who lack the T lymphocytes that develop into killer cells that destroy infected cells or become helper cells that communicate with other immune cells. X-linked severe combined immunodeficiency, most often diagnosed during the first year of life, allows organisms that do not affect people with healthy immune systems to cause frequent and life-threatening infections.

Complement deficiencies usually involve an absence of one or several of the proteins that contribute to the complement system's ability to attach to antibody-coated foreign invaders. In childhood or early adulthood, a complement deficiency can result in severe infections such as meningitis, or it can contribute to an autoimmune disease such as lupus erythematosus.

Phagocytic cell deficiencies result in the inability of cells that engulf and kill antibody-coated invaders to act efficiently to remove pathogens or infected cells from the body. Chronic granulomatous disease, the most severe form of phagocytic deficiency, usually appears in early childhood. It causes frequent and severe infections of the skin, lungs and bones, leaving swollen collections of inflamed tissue called granulomas.

In comparison to the secondary, the primary immunodeficiencies syndromes are rare.

Common conditions associated with *secondary immune deficiency* are adapted from Bonilla FA, Secondary immune deficiency due to immunosuppressive drugs and infections other than HIV (personal communication 2008):

- Immunosuppressive therapy
  - Cytotoxic chemotherapy for malignancy
  - Treatment of autoimmune disease
  - Bone marrow ablation prior to transplantation
  - Treatment or prophylaxis of graft vs host disease following bone marrow transplantation
  - Treatment of rejection following solid organ transplantation
- Microbial infection
  - Viral infection
    - HIV, AIDS
    - Measles
    - Herpes viruses
  - Bacterial infection (superantigens)

- Mycobacterial infection
- Parasitic infestation
- Malignancy
  - Hodgkin's disease
  - Chronic lymphocytic leukemia
  - Multiple myeloma
  - Solid tumors
- Disorders of biochemical homeostasis
  - Diabetes mellitus
  - Renal insufficiency/dialysis
  - Hepatic insufficiency/cirrhosis
  - Malnutrition
- Autoimmune disease
  - Systemic lupus erythematosus
  - Rheumatoid arthritis
- Trauma
  - Burns
- Environmental exposure
  - Radiation
    - Ionizing
    - Ultraviolet
  - Toxic chemicals
- Other
  - Pregnancy
  - Stress
  - Asplenia/hyposplenism
  - Allogeneic blood transfusion
  - Aging

A wide variety of so-called opportunistic infectious agents, many of which rarely cause infection in normal hosts, can cause these pneumonias, and often, more than one agent is involved. The mortality from these opportunistic infections is high. On the other hand, the list of differential diagnoses of such infiltrates is long and includes drug reactions, cardiac failure, and involvement of the lung by tumor or other underlying conditions. Table 13.2 lists some of the opportunistic agents according to their prevalence and whether they cause local or diffuse pulmonary infiltrates. The large group of immunocompromised patients sometimes is divided into AIDS and non-AIDS causes of immunosuppression. The types of infection to which HIV-positive patients become susceptible vary as cell-mediated immunity becomes less effective at eradicating viruses, fungi, protozea, and facultative intracellular bacteria, such as *Mycobacterium tuberculosis*. Knowledge of the CD4 lymphocyte count can thus be helpful for interpretation of radiologic images in AIDS patients (MARQUARDT and JABLONOWSKI 2003). Table 13.3 gives a short overview of the CD4 counts and corresponding infections.

As mentioned previously the radiographic patterns in most of the cases are not pathognomonic and the pat-

Table 13.2. Causes of pulmonary infiltrates in immunocompromised hosts (from Husain and Kumar 2005)

Causes of pulmonary infiltrates in immunocompromised hosts	
Diffuse infiltrates	**Focal infiltrates**
Common	*Common*
Cytomegalovirus	Gram-negative rods
Pneumocystis jiroveci	*Staphylococcus aureus*
Drug reaction	Aspergillus
	Candida
	Malignancy
Uncommon	*Uncommon*
Bacteria	Cryptococcus
Aspergillus	Mucor
Cryptococcus	*Pneumocystis jiroveci*
Malignancy	*Legionella pneumophila*

Table 13.3. Overview of the CD4 counts and corresponding infections

HIV – Complications at CD4 >500/mm^3	HIV – Complications at CD4 200–500/mm^3
Infectious	**Infectious**
Acute retroviral syndrome	Pneumococcal pneumonia
Candida vaginitis	Tuberculosis
	Herpes zoster
	Kaposis sarcoma
	Oral hairy leukoplakia (OHL)
	Oropharyngeal candidiasis (thrush)
Other	Non-Infectious
Generalized lymphadenopathy	Cervical carcinoma
Guillain-Barre (very rare)	Lymphomas
Vague constitutional symptoms	Immune thrombocytopenic purpura (ITP)

tern approach is limited by underlying and concomitant diseases, the severity and time factor of manifestation, and treatment. It is frequently impossible for the clinician to identify the causative organism of a pneumonic infiltrate. Narrowing of the etiologic differential diagnosis may be possible using *radiologic pattern* recognition and the integration with clinical and laboratory information. Although with pattern recognition, specific etiologic diagnoses can hardly ever be established, patterns help to classify groups of potentially underlying organisms.

As a general rule of thumb, localized segmental or lobar aveolar densities can be attributed to typical or atypical bacterial infections. Diffuse bilateral interstitial and/or interstitial alveolar infiltrates most commonly are caused by viruses, atypical bacteria, and protozoa. Micro-nodular disease is most often caused by miliary tuberculosis (miliary pattern), candidiasis, and histoplasmosis (small nodules), or viruses such as herpes or varicella zoster virus (diffuse nodules with hazy borders). Large, nodular lesions may represent bacterial abscesses, and in immuno-compromised patients, may be caused by invasive aspergillosis and nocardia.

In conclusion, the important tasks of imaging the lung with respect to pneumonia are:

- Detection of pulmonary abnormalities
- Support in narrowing the etiology or differential diagnosis
- Recognition of developing complications
- Demonstration of a therapeutic effect (however, radiographic patterns may change, even deteriorate with the immunologic status of the patient)

Looking at MRI for detection of pneumonia, the next part of this chapter is divided into a historical overview mentioning older and recent MR imaging concepts and a comparison of MRI with CT in the detection of pulmonary abnormalities suspicious for pulmonary infection.

13.4
MRI – Historical Overview and Imaging Concepts

In the beginning, MRI was an extension of traditional NMR spectroscopy in which the quantitative chemical analysis of a homogeneous sample is determined by the application of magnetic fields. Even in the 1970s and 1980s the use of MRI to diagnose the presence and extent of cancer was an active area of research. Another area of clinical interest was the use of proton MRI in the diagnosis of diseases, related to water content and

movement, such as edema, heart diseases, and circulation problems. Effective MRI section thicknesses at that time were approximately 1 cm (Partain et al. 1980).

James et al. (1982) concluded in a review that, because of its limited signal-to-noise ratio and inherent low sensitivity, MRI, in many respects, is not comparable to CT. But recognition that the information provided is fundamentally different from the attenuation of energy as in CT is conceptually important.

One of the first preliminary studies about MRI of the thorax was published by Gamsu et al. (1983). The study population consisted of 10 normal volunteers and 12 adult patients; 9 of these had advanced lung cancer, and 3 had nonmalignant lesions of the thorax. They were imaged with a 0.35-T superconducting magnet using spin-echo sequences, the individual sections were 7 mm thick and adjacent sections were separated by 5 mm. Ten patients underwent CT, and all underwent chest radiography. In conclusion of the results the authors found that hilar masses and lymphadenopathy were easily distinguished from blood vessels and hilar fat because of differences in T1 time. But the spin-echo images and the relaxation times did not show differences between tumor and consolidated lung tissue (Gamsu et al. 1983).

In 1984, 33 patients with a variety of chest abnormalities were examined at 0.6-T; 28 of the patients had proved malignant disease. In this study population Ross et al. (1984) found that MRI was considered to be as diagnostic as CT in determining abnormalities in 15. MR was superior to CT in one patient who had a right suprahilar carcinoma. CT proved superior to MRI in two patients. One patient had tracheal stenosis and one patient had an esophageal carcinoma. Another important result in this publication was the detection of disadvantages of MRI in chest imaging:

- Prolonged data acquisition time (the total time for an MR study of the chest averaged 1–1.5 h, vs 30 min for a CT examination)
- Relatively thick imaging section with associated partial volume averaging
- Failure to visualize calcium
- Pleural effusions were not easily characterized (Ross et al. 1984).

A more detailed comparison of MRI and CT for the staging of bronchogenic carcinoma was performed by Webb et al. (1985). They investigated 33 patients with histologically proved bronchogenic carcinoma at 0.35-T MR using multi-section spin-echo technique. Scanning was performed without electrocardiogram (ECG) gating. In comparison with CT, MRI provided comparable information regarding the presence and size of medi-

Table 13.4. Comparison of MRI and CT in 25 patients with chronic infiltrative lung disease (from Müller et al. 1992)

Findings	No. of Patients by Imaging Study			
	CT	T1	PD	T2
Vessels				
Central	25	25	24	24
Peripheral	25	25	18	3
Airways				
Lobar	25	25	25	25
Segmental	25	21	20	8
Subsegmental	25	8	5	4
Secondary pulmonary lobule				
Interlobular septum or vein	25	19	15	7
Centrilobular arteriole	25	11	5	1
Interstitial abnormality				
Reticulation	15	13	12	4
Honeycombing	10	9	6	0
Septal thickening	16	12	11	4
Nodules	6	5	6	5
Distribution of interstitial abnormalities				
Peribronchovascular	4	4	4	4
Peripheral	11	10	10	9
Diffuse	7	7	7	7
Patchy	4	5	5	4
Air-space abnormality				
Ground-glass opacity	18	19	18	17
Consolidation	5	5	5	5

astinal lymph nodes. Bronchial abnormalities were better seen on CT, primarily because of its better spatial resolution. Direct invasion of the mediastinum adjacent to a hilar mass was usually better demonstrated on MRI because of the ease with which tumor and mediastinal vessels could be distinguished. In three of four patients who had a surgically proved hilar mass with a peripheral obstructive pneumonia, the central tumor could be distinguished from collapsed peripheral lung on MR images performed with a repetition time (TR) of 2.0 s. The peripheral lung appeared more intense than tumor (Webb et al. 1985).

To find if it is possible to differentiate further various causes of pulmonary consolidation with MRI, Moore et al. (1986) analyzed patients with pulmonary edema, postobstructive pneumonitis, alveolar proteinosis,

Pneumocystis pneumonia, lobar nonobstructive pneumonia, pulmonary hemorrhage, and acute radiation pneumonitis. The study was performed with a 0.35-T MR scanner, using spin-echo pulse sequences with repetition times of 500 and 2000 ms and echo times (TE) of 28 and 56 ms. In summarizing the results, the authors could demonstrate that measuring T1 and T2 values the different entities showed considerable overlap. The two patients with pulmonary alveolar proteinosis showed much lower values of T1, which probably reflects the relative absence of water within the airspaces and the presence of lipoprotein. In general, T1 and T2 values increase in proportion to the water content of fluids or tissue, but they are also influenced by the presence of lipids and by interaction between water and both large and small molecules with which they come in contact (MOORE et al. 1986).

High-resolution computed tomography (HRCT) had become the gold standard in the evaluation of chronic infiltrative lung diseases and it was shown that it accurately reflects the pathologic abnormalities. The aim of a study from MÜLLER et al. (1992) was to compare MRI with HRCT in the assessment of these entities. All MR studies were performed on a 1.5-T MR imager. Cardiac-gated proton density-weighted and relatively T2-weighted images were obtained at two or three RR intervals. The slice thickness was 10 mm, with a 1- or 2-mm interslice gap. In comparison to this the CT scans were obtained by using 1.5-mm collimation scans, and 10-mm intervals. Table 13.4 summarizes the results.

As a result, MRI was consistently inferior in the anatomic assessment of lung parenchyma and in showing interstitial abnormalities, particularly fibrosis. Furthermore, areas of mild interstitial abnormalities seen on CT were often not apparent on MRI. But, on the other hand, MRI was comparable to CT in the assessment of air-space abnormalities. In all patients, areas with ground-glass opacities or air-space consolidation on CT corresponded to areas of increased signal intensity on MRI (MÜLLER et al. 1992).

Primack et al. noticed that the use of MRI in the assessment of infiltrative lung disease has been limited by the low proton density of lung parenchyma and by loss of signal due to motion and the difference in diamagnetic susceptibility of air and soft tissue. On the other hand, the presence of pulmonary infiltrates leads to a marked increase in signal intensity. This is due to both the increase in proton density and a decrease in magnetic susceptibility effects. They included 22 consecutive patients with idiopathic pulmonary fibrosis, sarcoidosis, extrinsic allergic alveolitis, Churg-Strauss syndrome, Wegener granulomatosis, necrotizing sarcoid granu-

lomatosis, hypersensitivity drug reaction, desquamative interstitial pneumonia-like drug reaction, silicosis, lymphangitic carcinomatosis, talcosis, and bronchiolitis obliterans organizing pneumonia (BOOP). All patients had MRI and open lung biopsy. Ten of the 12 patients with parenchymal opacification as the predominant abnormality on MRI had cellular infiltrates pathologically, while fibrosis was present in the other 2. This study demonstrated that the MRI findings correlate with the pathologic findings and that parenchymal opacification on MRI usually indicates an inflammatory process, and therefore potentially treatable disease. Localized areas of fibrosis were easier to identity on CT than on MRI. Again, as mentioned in previous studies, these authors found out that a major limitation of MRI in the assessment of infiltrative lung disease was the low spatial resolution compared with HRCT (PRIMACK et al. 1994).

One of the earlier studies that focused on contrast-enhanced pulmonary MRI was published by HARALDSETH et al. (1999). They reviewed different forms of contrast agent enhancement: MR perfusion imaging, contrast enhanced MR angiography, and MR ventilation imaging. In the clinical context of pneumonia they included 13 patients. The MR perfusion was obtained with a standard low flip-angle gradient-echo sequence with an inversion prepulse. The time-intensity curves after intravenous application of a gadolinium-based non-specific contrast agent showed that in pneumonic tissue there was a steep increase without first passage peak; the dynamics of the contrast agent passage was different from normal lung tissue (Fig. 13.1). The authors did not suggest replacement of chest X-rays for routine pneumonia diagnosis, but in cases where the differential diagnosis between pulmonary embolism and pneumonia were two main options, patients might benefit from an MR perfusion examination (HARALDSETH et al. 1999).

A more detailed description of MRI of the pulmonary parenchyma was published by KAUCZOR and KREITNER (1999). As a brief summary of the technical considerations the authors noticed the following three factors hampering the application of MRI to the lung and suggested the following strategies to resolve the problems:

1. *Low proton density*: This is valid for the normal lung parenchyma and especially for lung diseases with loss of tissue such as emphysema. In all other lung diseases, the amount of tissue, fluid, and/or cells is increased. The recommended investigation techniques are:

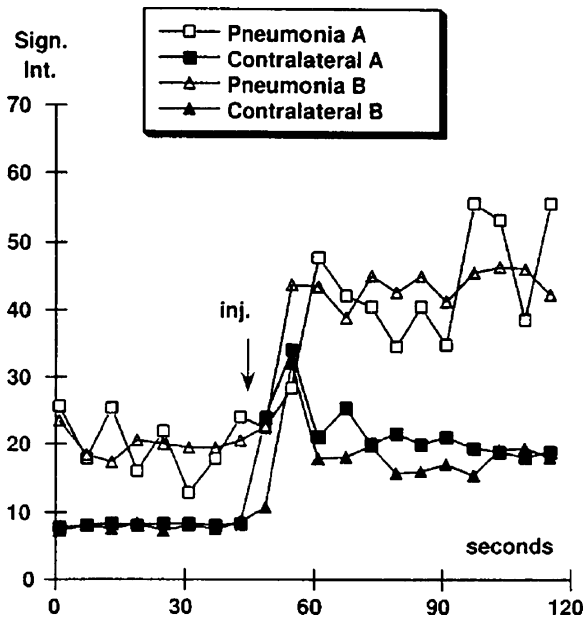   a) T1-weighted spin-echo sequences with short echo times (<7 ms)

Fig. 13.1. Time-intensity curves depicting the first passage in two patients with pneumonia; in the inflammatory tissue and in the contralateral lung (from HARALDSETH et al. 1999)

b) T1-weighted gradient-echo sequences, such as fast low-angle shot (FLASH), with short echo times (3 ms)
c) Higher number of acquisitions
d) Administration of contrast agents

2. *Signal loss due to physiological motion*:
   a) Breath-hold imaging with fast sequences like FLASH or half-Fourier acquired single-shot turbo spin echo (HASTE)
   b) Respiratory gating with navigating techniques, gating in expiration using a belt, and respiratory compensation using reordering of phase encoding
   c) ECG triggering

3. *Susceptibility artefacts because of the multiple air-tissue interfaces*: As mentioned previously these artefacts degrade imaging of normal lung tissue. After loss of air and concomitant increase of tissue, cells, or fluid significantly reduces the number of air-tissue interfaces and the degree of susceptibility artefacts:
   a) Use of short echo times for T1-weighted spin-echo or gradient-echo sequences
   b) Use of T2-weighted turbo-spin-echo (TSE) sequences or T2-weighted ultrafast TSE-sequences with high turbo factors

With regard to infiltrations, the authors concluded that MRI can be used for the detection and characterization of inflammatory pulmonary round infiltrates in immunocompromised patients. Post-contrast T1-weighted FLASH showed a strongly enhancing, ill-defined round infiltration (Fig. 13.2), and with HASTE sequence moderate signal intensity was found in a patient with bronchopneumonia (Fig. 13.3a–e) (KAUCZOR and KREITNER 1999).

GAETA et al. (2000) revisited the value of gadolinium-enhanced MRI in the evaluation of chronic infiltrative lung disease. They found out that the presence of enhancing lesions on gadolinium-enhanced T1-weighted MRI studies may a reliable indicator of inflammation and, consequently, indicates potentially treatable disease. Their study was performed on a 1.5-T scanner obtaining a spoiled gradient-echo T1-weighted sequence during full inspiration (TR 168 ms, TE 4.8 ms, FA 75°, slice thickness 5 mm) (GAETA et al. 2000).

Another topic in literature is the differentiation between benign and malignant nodular lesions of the lung. Growth factors and calcification pattern are only two of a noninvasive diagnostic armamentarium to separate benign from suspicious lesions, to avoid unnecessary invasive tests. To overcome the limitation of morphological features LI et al. (2000) included 62 patients to evaluated suspicious lung nodules with CT and dynamic Gd-DTPA enhanced MRI. Axial T1-weighted images (TR 500 ms, TE 10 ms) with a slice thickness of

Fig. 13.2. A 45-year-old male patient with invasive aspergillosis. Post-contrast T1-weighted FLASH (TR >200 ms, TE = 4 ms, FA = 80°) shows a strongly enhancing, ill-defined round infiltration (*arrow*) (from KAUCZOR and KREITNER 1999)
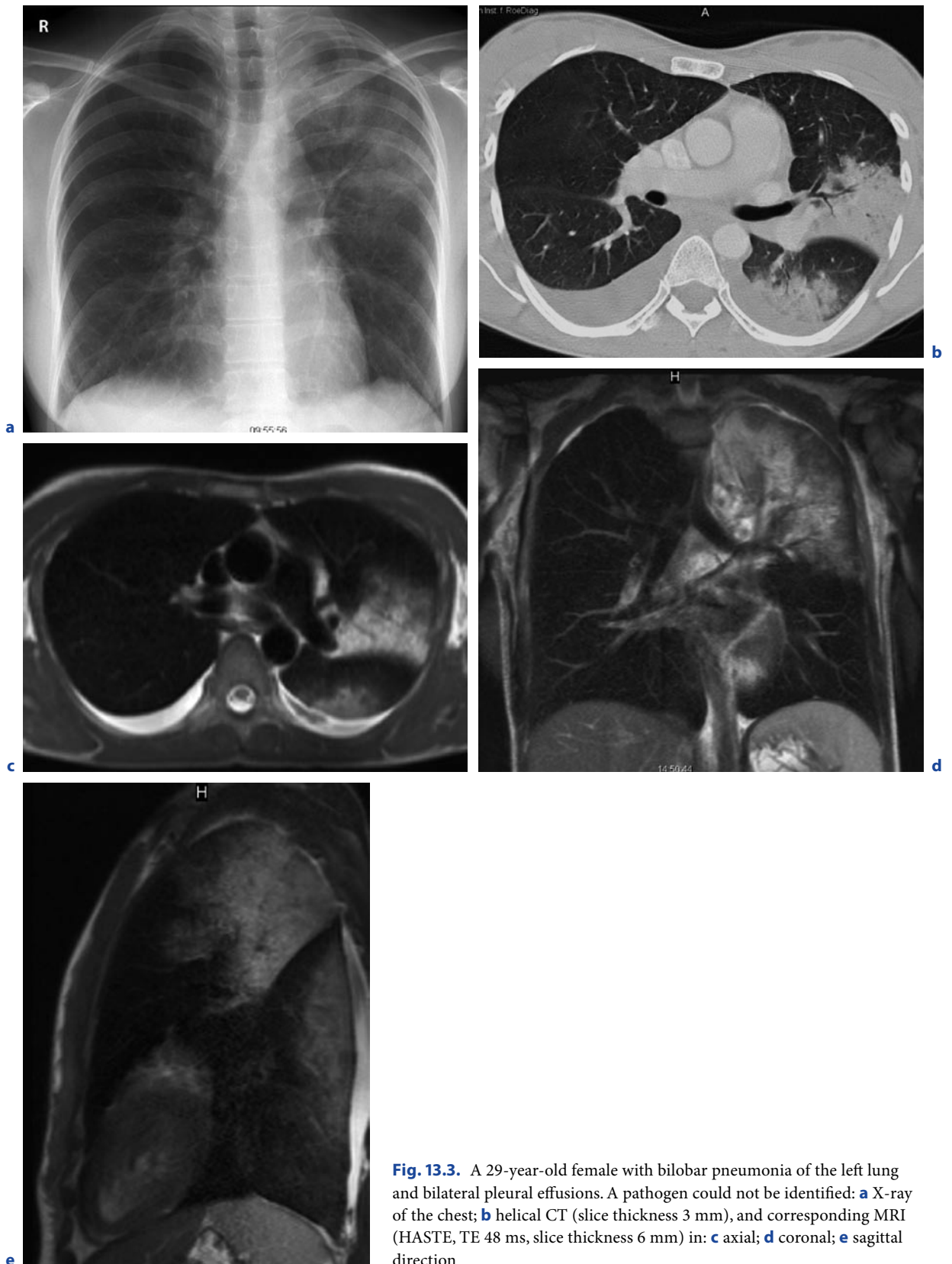
Fig. 13.3. A 29-year-old female with bilobar pneumonia of the left lung and bilateral pleural effusions. A pathogen could not be identified: **a** X-ray of the chest; **b** helical CT (slice thickness 3 mm), and corresponding MRI (HASTE, TE 48 ms, slice thickness 6 mm) in: **c** axial; **d** coronal; **e** sagittal direction

5 mm at 0, 15, 45, 75, 110, and 140 s, and 3, 5, 8, and 10 min were obtained. Additional T2-weighted images (TR 3000 ms, TE 80 ms) were obtained before contrast application. After correlation with pathological findings they found out that nodular fibrosis, inflammatory granulomas, cryptoccocoma and inflammatory pseudotumor had a more or less low rate of contrast uptake. On the other hand, focal organizing pneumonia and sclerosing hemangioma had a significant and early enhancement. Taking into account that malignant nodules are characterized by a fast increase in signal intensity during the first pass of the contrast agent (Gückel et al. 1996), at least some nodular lesions could be excluded to be malignant with dynamic MR (Li et al. 2000).

That further developments in sequence design will have potential in imaging the lung parenchyma was investigated by Bader et al. (2002) and Rupprecht et al. (2002). Bader et al. (2002) included 20 patients with pulmonary diseases comprising non-small-cell, and bronchioalveolar carcinomas, endobronchial mucoepidermoid carcinoma, metastases, pneumonia, Wegener's granulomatosis, chronic obstructive pulmonary disease, arterio-venous malformation, and bronchogenic cyst. MRI studies were performed at 1.5 T before and after administration of gadolinium using a modified volumetric interpolated breath-hold examination (VIBE) (TR 4.6 ms, TE 1.8 ms, FA 15°, effective slice thickness 4 mm). Their results demonstrated that reproducible high image quality with effective suppression of artefacts, high resolution, and visualization of gadolinium enhancement could be obtained. Rupprecht et al. (2002) performed a study without contrast agent and investigated a steady-state free precession sequence (true FISP) as a potential alternative to the conventional X-ray in pediatric patients with suspected pneumonia. A true FISP sequence was chosen because of its high spatial resolution and signal-to-noise ratio (S/N) in fluid- and thus T2-dominated infectious pulmonary disease. To overcome breathing artefacts in this particular patient group and to increase the S/N ratio they obtained slice thicknesses of 30–55 mm at a 0.2-T low-field MR system. The true FISP sequence had the following parameters: TR 6 ms, TE 3 ms, FA 90°. The acquisition time for a triple slice scan was 4.8 s, and the door-to-door time was between 10 and 15 min. All pathological findings in the conventional chest X-ray could be identified in the corresponding MR investigation and the MRI was superior in demonstrating pleural and pericardial effusions. Two small retrocardial pneumonic infiltrates were noted in the MRI only. The authors concluded that this technique could represent an alternative to the conventional chest X-ray (Rupprecht et al. 2002). Such an alternative might be of special interest in children with Nijmegen-Breakage-Syndrome. This entity is an autosomal recessive chromosomal instability syndrome, characterized by microcephaly, growth retardation, skin abnormalities, immunodeficiency, radiation sensitivity, and a strong predisposition to lymphoid malignancy. Because of their sensitivity to ionizing radiation X-ray and CT examination should be avoided (Alibek et al. 2007).

Whether it is possible not only to detect but also to quantify pulmonary lesions due to pneumococcal pneumonia was investigated in a murine model by Marzola et al. (2005). Infection was induced in a group of mice (N = 5) by intranasal administration of a suspension containing Streptococcus pneumoniae, and a group of noninfected animals (N = 5) was used as a control group. Axial, ECG-gated, spoiled GRE images with 1.2 mm slice thickness were acquired with a 4.7-T scanner. After sacrifice and histological evaluation a good concordance with regard to the anatomical localization and a good correlation between the volume of the pneumoniae by histology and MRI was found (Marzola et al. 2005).

Another interesting experimental study was published by Tournebize et al. (2006). The aim of this work was to prove if MRI is able to provide spatio-temporal visualization of edema and inflammation caused by *Klebsiella pneumoniae* induced pneumonia in mice. The study was performed with a 7-T scanner. After inoculation with avirulent and virulent strains of Klebsiella, treatment by bactericidal doses of antibiotics was initiated. Images were acquired up to 8 days post infection. The virulent strain caused an intense inflammation within 2 days in the whole lungs, while an avirulent strain did not show significant changes. The increase in cell density accompanied with extravascular leakage results in an increase in high water content detectable by MRI. After treatment with antibiotics the inflammation disappeared after a week. The lesions observed by MRI correlated with the damage seen by histological analysis. In summary MRI allows observing the appearance and regression of inflammation (Tournebize et al. 2006).

The next important topic was the investigation of the sensitivity of MRI in detecting alveolar infiltrates. To provide reliable data, Biederer et al. (2002) performed an experimental study using porcine lung explants and a dedicated chest phantom to evaluate the signal intensity of artificial alveolar infiltrates with T1- and T2-weighted MRI sequences. Ten porcine lung explants were examined with MRI at 1.5 T before and after intra-tracheal instillation of either 100 or 200 ml gelatine-stabilised liquid to simulate alveolar infiltrates. Control studies were acquired with helical CT. Table 13.5 summarizes the applied MR sequences.

After administration of the gelatine-stabilised liquid, the CT images demonstrated patchy areas of ground-glass opacities in both lungs. The 2D and 3D T1-weighted sequences could not sufficiently visualize the infiltrates. In contrast the T2-weighted sequences showed clearly visible infiltrates with an increase in signal intensity of approximately 30% at 100 ml (p <0.01) and 60% at 200 ml (p <0.01). For practical reasons: T2-weighted sequences can be highly recommended for the delineation of infiltrates in the lung. T1-weighted sequences without intravenous application of contrast agents are not sufficient for this task. Because of the extremely different acquisition times between HASTE and the T2-TSE, the HASTE sequence has to be preferred. Table 13.6 overviews the results in detail (Biederer et al. 2002).

After these historical and technical developments it is necessary to evaluate the potential of MRI in detecting pneumonia in the immunocompromised patient. Especially in this particular group of patients, pneumonia is an important cause of morbidity and mortality. The imaging of infiltrates is very challenging, because the immunosuppression decreases the response of the lung to infectious agents. On the other hand, the patterns of pneumonia are highly variable and depend on multiple factors, like underlying diseases, time course, treatment, e.g. By now, a considerable proportion of pulmonary fungal infections is not diagnosed ante mortem in cancer patients. In addition, especially patients after bone marrow transplantation are often younger and repetitive CT examinations carry an additional radiation burden.

Leutner et al. (2000) tried to find out how MRI compares with CT regarding the depiction of typical features of pneumonia and the detectability of lesions. MR studies was performed with a 1.5-T system and the imaging protocol consisted of a transversal T2-weighted ultrashort turbo spin-echo sequence (TR 2000–4000 ms, TE 90 ms, slice thickness 6 mm, and six numbers of excitation). In comparison to helical CT (slice thickness 8 mm) they evaluated presence, number, and location of pulmonary infiltrates (nodular, reticular, cysts, cavitation, consolidation, and ground-glass infiltration). In summary, most of the CT and MR examinations (75%) were rated as showing identical results concerning not only the number but also the morphology of different lesions that were due to opportunistic pneumonia. In addition, MRI was able to differentiate between consolidation and ground-glass infiltration (Leutner et al. 2000).

13.5

MRI – Comparison with CT

The advent of multislice CT and the implementation of parallel imaging in MRI pushed the limits towards new possibilities with regard to examination volume, time, and slice thickness. Multislice CT offers the opportunity

Table 13.5. Summary of the applied sequences for the investigation of the chest phantom (from Biederer et al. 2002)

Sequence	2D-GRE	3D-GRE (VIBE)	3D-GRE (VIBE)	HASTE	HASTE	T2-TSE
Weighting	T1	T1	T1	T2	T2	T2
Slice orientation	Axial	Axial	Coronal	Axial	Coronal	Axial
TR/TE (ms)	100/2.2	4.5/1.9	4.5/1.9	2000/43	2000/43	3000/120
FA	50	12	12	180	180	120
FOV (mm)	350	350	350	350	350	350
Matrix	222 × 256	502 × 512 interpolated	502 × 512 interpolated	224 × 256	224 × 256	270 × 512
Slice thickness (mm)	6	2.5 interpolated	2.5 interpolated	7	7	8
Slice per acquisition	19	32	32	7	7	12
Acquisition-time	23 s	23 s	23 s	18 s	18 s	4 min 51 s

Table 13.6. Measurement of signal intensities (SI), calculation of standard deviations (SD) and signal-to-noise ratios before (native) and after instillation of liquid (with infiltration) (adapted from Biederer et al. 2002)

Sequence	Infiltration with 100 ml				Infiltration with 200 ml			
	SI	SD	S/N	Increase (%)	SI	SD	S/N	Increase (%)
2D-GRE								
Native	31.28	3.2	1.15		30.2	2.3	1.11	
With infiltration	31.51	3.3	1.16	0.74 p = 0.32	31.8	2.6	1.12	5.6 p < 0.01
3D-GRE								
Native	17.0	1.11	1.13		17.2	1.16	1.16	
With infiltration	17.3	1.36	1.15	2.2 p = 0.02	18.0	1.16	1.22	4.4 p < 0.01
T2-HASTE								
Native	94.9	18.6	3.62		96.2	17.6	3.74	
With infiltration	127	21.2	5.03	34.4 p < 0.01	153	20.0	6.0	60.5 p < 0.01
T2-TSE								
Native	14.13	2.8	1.39		14.3	3.0	1.34	
With infiltration	18.41	3.7	1.85	30.3 p < 0.01	23.4	3.5	2.23	63.4 p < 0.01
CT (in HU)								
Native	150	24.3	16.1		139	21.2	13.9	
With infiltration	167	25.3	17.3	11.2 p = 0.02	234	10.4	23.4	68.4 p < 0.01

to investigate the entire lung with 1 mm slice thickness or less in much shorter than 1 min. Parallel imaging in MRI reduced dramatically the examination time that makes acquisition of the lungs in a few seconds possible.

Thin-section helical CT is the gold standard for the evaluation of the lung even for very subtle lesions like small ground-glass opacities around lung nodules. That means, to classify the value of MRI of the lung, studies are necessary that compare MRI with the best CT techniques that are available nowadays.

Eibel et al. (2006b) performed a study where they investigated pulmonary abnormalities in 30 immunocompromised patients with parallel MRI and thin-section helical CT. Table 13.7 summarizes the MR examination protocol for the applied HASTE sequence. It was not the intention of this study to investigate the lung comprehensively. In order not to exceed 1 min examination time, only the HASTE sequence was selected. The resulting in-room-time was not more than 10 min. The motivation was that MRI can only serve as a real alternative to CT, when the examination time is comparable.

One of the inclusion criteria for this study was an X-ray of the chest that was either normal or did not show abnormalities suggestive of pulmonary infection. Ill-defined nodules, ground-glass opacity areas, and consolidations, their location and distribution, and their lesion characteristics (e.g. margin contour, cavitation, calcification) were systematically analyzed. Twenty-two patients had pulmonary abnormalities on CT. In 21 (95%) patients, pneumonia was correctly diagnosed with MRI. One false-negative finding occurred in a patient with ill-defined nodules smaller than 1 cm at CT. One false-positive finding with MR was the result of blurring and respiratory artefacts. That results in a sensitivity of MRI in comparison to 1-mm CT slices of 95%, specificity of 88%, positive predictive value of 95%, and a negative predictive value of 88% (Eibel et al. 2006a). In the

Fig. 13.4 A 76-year-old patient with myelodysplasia suffering from *Pneumocystis jiroveci* pneumonia (from Eibel et al. 2006a): **a** thin-section CT above the level of the carina. Ground-glass opacity is the predominant finding in the ventral portion of the left upper lobe. Please note also the more subtle lesions in the dorsal parts of the both upper lobes; **b** axial HASTE-sequence at the same level (TE 27 ms). All lesions in the upper lobes are easily detectable
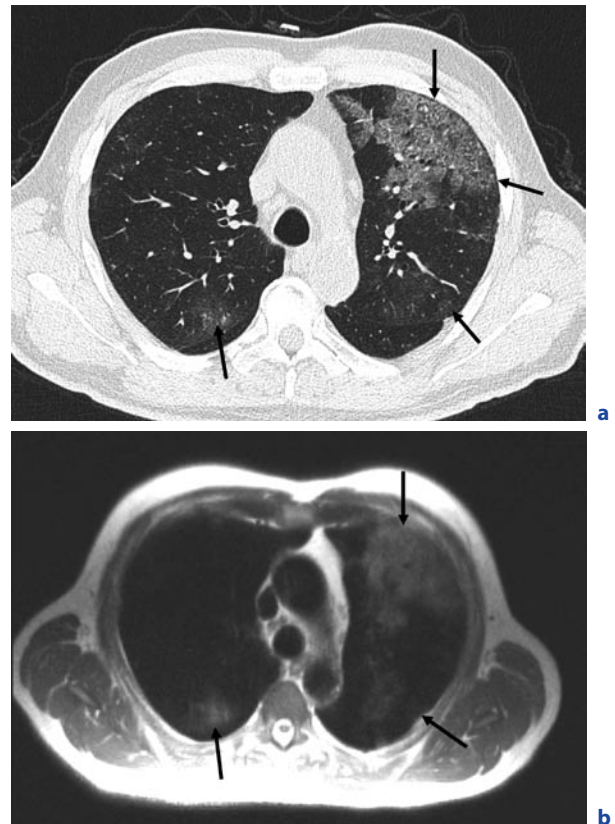
detection of ground-glass opacity areas (Fig. 13.4), consolidations (Fig. 13.5), and pleural effusion, MRI seems to be equal to thin-section CT. But the overall detection rate of nodules with MRI was only 72% (186/259). Detailed analyses found out that all nodules larger than 10 mm were reliably detected. The mean size of nodular lesions not found with MRI was 4 mm. This difference likely relates to the section thickness used with CT (1 mm) and MR imaging (6 mm). After this study the authors came to the conclusion that pulmonary imaging for the detection and quantification of infiltrates is highly reliable with modern MR scanners (Eibel et al. 2006b).

Despite these encouraging results it is important to keep in mind is that CT has to be preferred in the detection of calcification, which can indicate some special disease entities and can be a sign of pulmonary scarring.

13.6
Morphology of Different Types of Pneumonia in MR Imaging

Before summarizing briefly the different MR features of pneumonia, already mentioned in the paragraphs before, the following statements are valid for MR imaging of pneumonia:

- Nodules larger than 1 cm in diameter, consolidations and ground-glass opacifications are detectable on MR images with a nearly identical sensitivity and accuracy with regard to lesion size and contour compared to CT. Obviously the definition of nodule, consolidation and ground-glass according to the Fleischner Society seems to be valid even for MRI (Hansell et al. 2008).
- With MR images it might be more challenging or even impossible to delineate small nodules (<10 mm) and small areas of air or calcifications

Table 13.7. Parameters of the HASTE sequence, applied in the study of Eibel et al. (2006b)

Magnet	1.5-T
TR	440 ms
TE	27 ms
Bandwidth	488 Hz/pixel
Echo spacing	3.76 ms
Slice thickness	6 mm
Gap	50%
FOV	256 × 256 (axial) 320 × 256 (coronal and sagittal)
Modus	Interleaved
Acquisition	GRAPPA
iPAT-factor	2 (24 reference lines)
Examination time for the entire lungs	2–3 × 15 s (per direction)

Fig. 13.5. A 45-year-old male with chronic lymphatic leukemia, suffering now from angioinvasive aspergillosis (from EIBEL et al. 2006a): **a** thin-section CT below the level of the carina shows a consolidation in the left lower lobe (*black arrow*), ground-glass opacity in the lingular lobe adjacent to the fissure (*white arrow*), and both-sided pleural effusions. Please note also the subtle lesion in the right lower lobe adjacent to the spine (*short arrow*); **b** axial; **c** coronal; **d** sagittal HASTE. The pathologic findings are again comprehensively delineated by MRI, even the subtle lesion in the left lower lobe adjacent to the spine (*arrow*)

within lung nodules or consolidations in comparison to thin-section helical CT.

In Table 13.8 the most common and important features of pneumonia on MR images and the likely causative organisms are summarized.

Fungal pneumonia is an important topic, necessary to go a little bit more into detail, especially when dealing with MR imaging. Some organisms like *Histoplasma capsulatum* and *Coccidioides immitis* are primary pathogens, but are found only in specific geographic areas. On the other hand, organisms like Aspergillus and Candida species are opportunistic agents that affect patients which already suffer from an underlying pulmonary disease or are immunocompromised. As invasive organisms the latter can cause sever tissue destruction and can influence the clinical outcome dramatically.

The pathogenesis of Aspergillus infection is complex, but worthy to know is the fact that this fungus causes necrosis in lung parenchyma due to extensive vascular permeation and occlusion of small to medium arteries. This permeation and especially the separation of necrotic lung from viable parenchyma in the recovery phase of the patient can cause life-threatening intra-alveolar hemorrhage.

Because of the different therapeutic approaches in patients with fungal pneumonia and because of the high morbidity and mortality in immunosuppressed patients

Table 13.8. MRI findings and corresponding likely causative organisms

MRI finding	Likely causative organisms
Lobar consolidation = Lobar pneumonia	*Streptococcus pneumoniae, Klebsiella pneumoniae, Legionella pneumophilia, Mycoplasma pneumoniae*
Patchy, sometimes bilateral interlobular consolidation = Bronchopneumonia	Streptococci, gram-negative bacilli, Legionella, anaerobes, virus
Ground-glass opacification and reticular pattern = Interstitial pneumonia	Virus, *Mycoplasma pneumoniae, Pneumocystis jiroveci* (Fig. 13.4)
Cavitation	Staphylococcus aureus, *Mycobacterium tuberculosis*, gram-negative bacilli, anaerobic bacteria
Round consolidation, halo, air-crescent sign, reverse target sign	*Aspergillus fumigatus* (Fig. 13.5)

with invasive aspergillosis it is necessary to know the signs of this type of infection in imaging studies:

- Single or multiple nodular infiltrates
- Nodule with halo phenomenon
- Homogeneous consolidation in segmental or sub-segmental spread
- Cavitation (air crescent sign)
- Reverse target sign

The ground-glass attenuation surrounding some of the nodules is termed as halo. Histopathologic studies delineated that the cause for this finding is hemorrhage around the nodule. With MR the halo sign is clearly detectable and thus can help to differentiate the causative agents. Air crescent is a finding more common detectable in the recovery phase and relates to resorption of necrotic tissue in the periphery of the lesion or to retraction of the sequestrum from viable lung parenchyma (KIM et al. 2001). This crescent like air collection is associated with a higher risk of massive hemoptysis.

BLUM et al. (1994) observed another characteristic feature of necrotizing pneumonia. On T2-weighted images higher signal intensity in the center combined with comparatively lower signal intensity in the rim outlined a characteristic feature that they called "reverse target sign". While the halo phenomenon is strongly suggestive of invasive aspergillosis in its early course, the reverse target sign is detectable in later stages. Probably because of the excellent soft-tissue contrast on MR imaging, LEUTNER et al. (2000) found that this issue is superior to contrast-enhanced CT in diagnosing necrotizing pneumonia.

Up to now, no comprehensive study compared the sensitivity and specificity of different imaging modalities for the diagnosis of invasive aspergillosis. BLUM et al. (1994) found out that MRI may be of diagnostic value in later stages of the disease and for the follow-up of nodular infiltrates on unknown etiology in immunocompromised patients. So, further studies are necessary to lower the high mortality of angioinvasive aspergillosis by making the diagnosis earlier and with a higher reliability.

13.7
Protocol

In this last paragraph a short protocol recommendation (Table 13.9) is listed, confirmed and illustrated by an upper lobe pneumonia (Fig. 13.6).

The T2-weighted HASTE sequence is the workhorse, necessary for detection and characterization of infectious lesions of the lung. Performing only the topogram and the axial HASTE in patients which are severely ill and breathless, the investigation time is below 2 min. The T1-weighted FLASH sequence with and without intravenous application of gadolinium is helpful for further characterization of infiltrates. This extends the investigation time to 15 min. The STIR and TrueFISP sequences can give additional information selected cases, but are not required in routine settings.

Table 13.9. Suggested investigation protocol at a 1.5-T MR scanner (Avanto, Siemens Medical Systems, Erlangen, Germany)

Sequence	Type	Weighting	Slice orientation	TR (ms)	TE (ms)	Flip angle	FS	Slice thickness (mm)	Gd IV
Topogram									
HASTE	SE	T2	Axial	1000	84	180		6	
		T2	Coronal	1000	84	180		6	
		T2	Sagittal	1000	84	180		6	
FLASH 2D	GE	T1	Axial	118	2	70		6	
		T1	Coronal	78	2	70	+	6	
STIR*	SE/IR	T2	Axial	3980	100	150	+	6	
TrueFISP*	SS	T2	Axial	3	1	60		6	
		T2	Coronal	3	1	60		6	
FLASH 2D	GE	T1	Axial	118	2	70	+	6	+
		T1	Coronal	78	2	70	+	6	+

Abbreviations: FLASH (Fast Low Angle Shot), Gd IV (Gadolinium intravenously), GE (Gradient Echo), FS (Fat Saturation), HASTE (Half fourier Acquisition Single shot Turbo spin Echo), IR (Inversion Recovery), SE (Spin Echo), SS (steady state), STIR (Short TI Inversion Recovery), TE (time to echo), TR (repetition time), TrueFISP (True Fast Imaging with Steady state Precession), *(not required in routine settings)

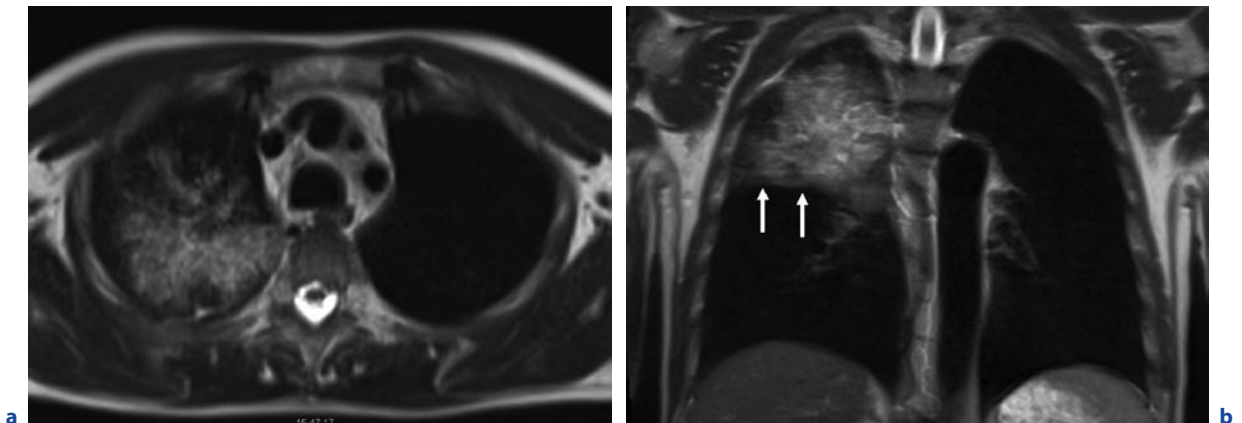**Fig. 13.6.** A 51-year-old male with right upper lobe pneumonia (Streptococcus): **a** axial HASTE. Consolidation with surrounding ground-glass in the right upper lobe; **b** coronal HASTE. The horizontal fissure (*arrows*) is not exceeded by the pneumonia; **c–h** *see next page*
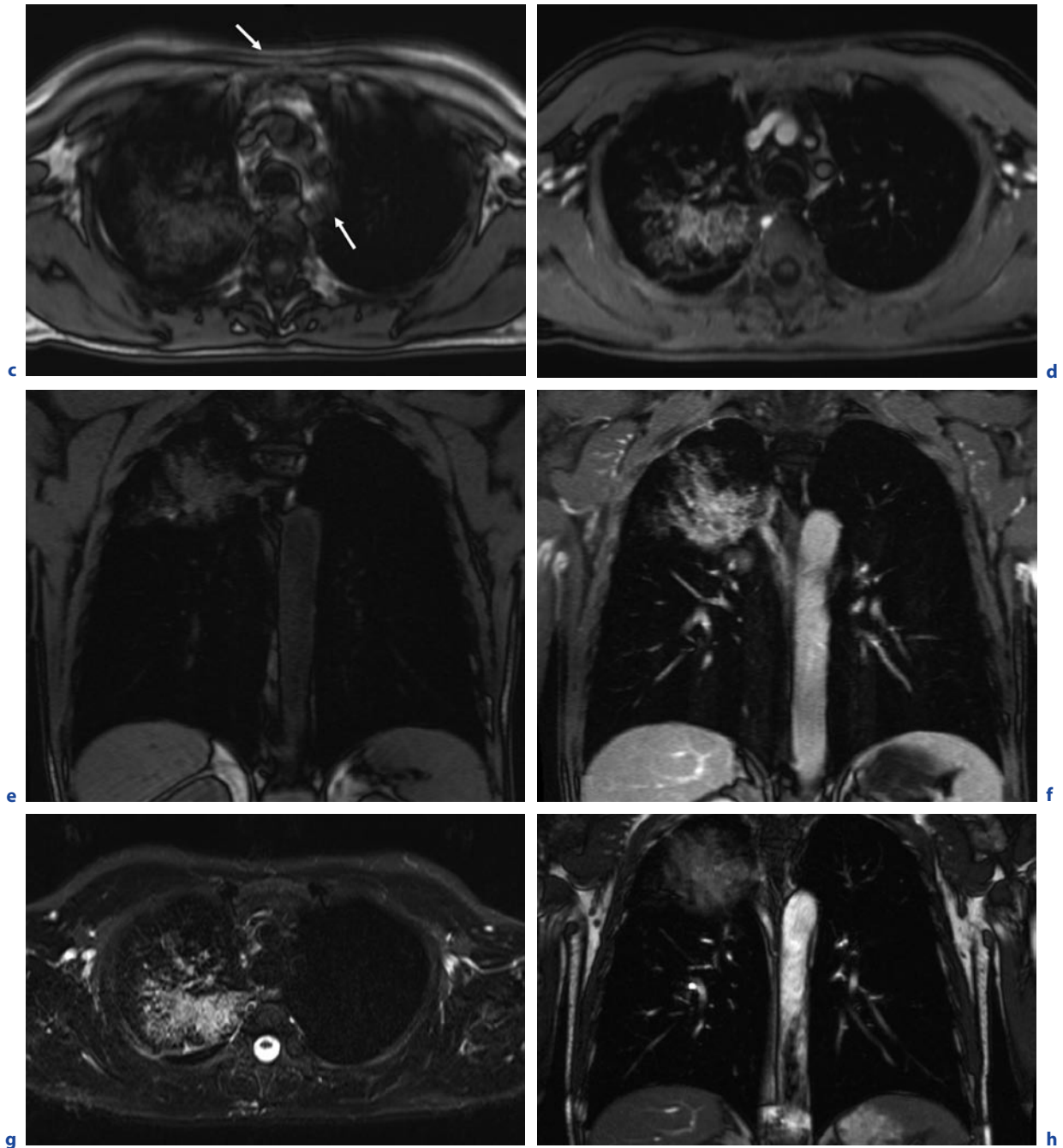
Fig. 13.6. (*continued*) A 51-year-old male with right upper lobe pneumonia (Streptococcus): **c** axial FLASH without fat saturation, not contrast enhanced. Without intravenous contrast application no additional information is given by this sequence in comparison to the HASTE sequence. Note the higher degree of artefacts in the mediastinum and chest wall (*arrows*); **d** axial FLASH with spectral fat saturation after delivery of 14 ml gadolinium IV. As a result of infection a significant enhancement is visualized; **e** coronal FLASH with spectral fat sat-uration, before intravenous contrast administration; **f** coronal FLASH, after gadolinium; **g** axial STIR. The edema is clearly detectable in the right upper lobe pneumonia, but the degree of artefacts and noise is higher in comparison to the HASTE se-quence; **h** coronal TrueFISP. The vessels are clearly detectable. So this sequence can be an alternative to the contrast enhanced FLASH to delineated adjacent vasculature. The pneumonia it-self is not better appreciable in comparison to the HASTE and contrast enhanced FLASH

References

Alibek S, Holter W, Staatz G (2007) The radiosensitive child: pulmonary MR tomography in EBV-induced lymphoproliferation in Nijmegen-breakage syndrome. FortschrRöntgenstr 179:1075–1077

Bader TR, Semelka RC, Pedro MS, Armao DM, Brown MA, Molina PL (2002) Magnetic resonance imaging of pulmonary parenchymal disease using a modified breath-hold 3D gradient-echo technique: initial observations. J Magn Reson Imaging 15:31–38

Biederer J, Busse I, Grimm J, Reuter M, Muhle C, Freitag S, Heller M (2002) Sensitivity of MRI in detecting alveolar infiltrates: experimental studies. FortschrRöntgenstr 174:1033–1039

Blum U, Windfuhr M, Buitrago-Tellez C, Sigmund G, Herbst EW, Langer M (1994) Invasive pulmonary aspergillosis. MRI, CT, and plain radiographic findings and their contribution for early diagnosis. Chest 106:1156–1161

Campbell GD, Niederman MS, Broughton WA et al. (1996) Hospital-acquired pneumonia in adults: diagnosis, assessment of severity, initial antimicrobial therapy, and preventative strategies: a consensus statement. Am J Resp Crit Care Med 153:1711–1725

Cook DJ, Walter SD, Cook RJ et al. (1998) Incidence of and risk factors for venilato-associated pneumonia in critically ill patients: results from a multicenter prospective study on 996 patients. Ann Intern Med 129:433–440

Craven DE, Steger KA (1995) Epidemiology of nosocomial pneumonia. New perspectives on an old disease. Chest 108:1S–16S

Eibel R, Herzog P, Dietrich O, Rieger C, Ostermann H, Reiser M, Schoenberg S (2006a) Magnetic resonance imaging in the evaluation of pneumonia. Radiologe 46:267–270, 272–274

Eibel R, Herzog P, Dietrich O, Rieger CT, Ostermann H, Reiser MF, Schoenberg SO (2006b) Pulmonary abnormalities in immunocompromised patients: comparative detection with parallel acquisition MR imaging and thin-section helical CT. Radiology 241:880–891

Fagon JY, Chastre J, Hance AJ, Domart Y, Trouillet JL, Gibert C (1993) Evaluation of clinical judgment in the identification and treatment of nosocomial pneumonia in ventilated patients. Chest 103:547–553

Gaeta M, Blandino A, Scribano E, Minutoli F, Barone M, Andò F, Pandolfo I (2000) Chronic infiltrative lung diseases: value of gadolinium-enhanced MRI in the evaluation of disease activity–early report. Chest 117:1173–1178

Gamsu G, Webb WR, Sheldon P, Kaufman L, Crooks LE, Birnberg FA, Goodman P, Hinchcliffe WA, Hedgecock M (1983) Nuclear magnetic resonance imaging of the thorax. Radiology 147:473–480

Gückel C, Schnabel K, Deimling M, Steinbrich W (1996) Solitary pulmonary nodules: MR evaluation of enhancement patterns with contrast-enhanced dynamic snapshot gradient-echo imaging. Radiology 200:681–686

Hansell DM, Bankier AA, MacMahon H, McLeod TC, Müller NL, Remy J (2008) Fleischner Society: glossary of terms for thoracic imaging. Radiology 246:697–722

Haraldseth O, Amundsen T, Rinck PA (1999) Contrast-enhanced pulmonary MR imaging. MAGMA 8:146–153

Husain AN, Kumar V (2005) The lung. In: Klatt EC, Kumar V (eds) Robbins and Cotran pathologic basis of disease, 7th edn. Elsevier Saunders, pp 711–772

James AE Jr, Partain CL, Holland GN, Gore JC, Rollo FD, Harms SE, Price RR (1982) Nuclear magnetic resonance imaging: the current state. AJR Am J Roentgenol 138:201–210

Kauczor HU, Kreitner KF (1999) MRI of the pulmonary parenchyma. Eur Radiol 9:1755–1764

Kim MJ, Lee KS, Kim J, Jung KJ, Lee HG, Kim TS (2001) Crescent sign in invasive pulmonary aspergillosis: frequency and related CT and clinical factors. J Comput Assist Tomogr 25:305–310

Leutner CC, Gieseke J, Lutterbey G, Kuhl CK, Glasmacher A, Wardelmann E, Theisen A, Schild HH (2000) MR imaging of pneumonia in immunocompromised patients: comparison with helical CT. AJR Am J Roentgenol 175:391–397

Li F, Sone S, Maruyama Y, Takashima S, Yang ZG, Hasegawa M, Honda T, Yamanda T, Kubo K (2000) Correlation between high-resolution computed tomographic, magnetic resonance and pathological findings in cases with non-cancerous but suspicious lung nodules. Eur Radiol 10:1782–1791

Marquardt T, Jablonowski H (2003) Opportunistic diseases. Risk can be estimated. MMW Fortschr Med 145:33–37

Marzola P, Lanzoni A, Nicolato E, Di Modugno V, Cristofori P, Osculati F, Sbarbati A (2005) (1)H MRI of pneumococcal pneumonia in a murine model. J Magn Reson Imaging 22:170–174

McEachern R, Campbell GD Jr (1998) Hospital-acquired pneumonia: epidemiology, etiology, and treatment. Infect Dis Clin North Am 12:761–779

Moore EH, Webb WR, Muller N, Sollitto R (1986) MRI of pulmonary airspace disease: experimental model and preliminary clinical results. AJR Am J Roentgenol 146:1123–1128

Müller NL, Mayo JR, Zwirewich CV (1992) Value of MR imaging in the evaluation of chronic infiltrative lung diseases: comparison with CT. AJR Am J Roentgenol 158:1205–1209

Niederman MS (2004) Pneumonia, including community-acquired and nosocomial pneumonia. In: Crasp JD, Glassroth J, Karlinsky J, King TE (eds) Baum's textbook of pulmonary diseases, 7th edn. Lippincott Williams and Wilkins, pp 425–454

Niederman MS, Mandell LA, Anzueto A et al. (2001) Guidelines for the management of adults with community-acquired lower respiratory tract infections: Diagnosis, assessment of severity, antimicrobial therapy and prevention. Am J Resp Crit Care Med 163:1730–1754

Partain CL, James AE, Watson JT, Price RR, Coulam CM, Rollo FD (1980) Nuclear magnetic resonance and computed tomography: comparison of normal human body images. Radiology 136:767–770

Primack SL, Mayo JR, Hartman TE, Miller RR, Müller NL (1994) MRI of infiltrative lung disease: comparison with pathologic findings. J Comput Assist Tomogr 18:233–238

Prod'hom G, Leuenberger P, Koefer J et al. (1994) Nosocomial pneumonia in mechanically ventilated patients receiving antacid, ranitidine, or sucralfate as prophylaxis for stress ulcer: a randomized controlled trial. Ann Intern Med 120:653–662

Rello J, Paiva JA, Baraibar J et al. (2001) International Conference for the Development of Consensus on the Diagnosis and Treatment of Ventilator-associated Pneumonia. Chest 120:955–970

Rosenow EC III (1990) Diffuse pulmonary infiltrates in the immunocompromised host. Clin Chest Med 11:55–64

Ross JS, O'Donovan PB, Novoa R, Mehta A, Buonocore E, Mac Intyre WJ, Golish JA, Ahmad M (1984) Magnetic resonance of the chest: initial experience with imaging and in vivo T1 and T2 calculations. Radiology 152:95–101

Rupprecht T, Böwing B, Kuth R, Deimling M, Rascher W, Wagner M (2002) Steady-state free precession projection MRI as a potential alternative to the conventional chest X-ray in pediatric patients with suspected pneumonia. Eur Radiol 12:2752–2756

Springhouse (2007) Professional guide to disease. An up-to-date encyclopedia of illnesses, disorders, and injuries and their treatments. Lippincott Williams and Wilkins

Tournebize R, Doan BT, Dillies MA, Maurin S, Beloeil JC, Sansonetti PJ (2006) Magnetic resonance imaging of Klebsiella pneumoniae-induced pneumonia in mice. Cell Microbiol 8:33–43

Webb WR, Jensen BG, Sollitto R, de Geer G, McCowin M, Gamsu G, Moore E (1985) Bronchogenic carcinoma: staging with MR compared with staging with CT and surgery. Radiology 156:117–124